Nascent transcript analysis of glucocorticoid crosstalk with TNF defines primary and cooperative inflammatory repression

Sarah K. Sasse, Margaret Gruca, Mary A. Allen, et al.

Genome Res. 2019 29: 1753-1765 originally published online September 13, 2019
Access the most recent version at doi:10.1101/gr.248187.119

Research

Nascent transcript analysis of glucocorticoid crosstalk with TNF defines primary and cooperative inflammatory repression

Sarah K. Sasse,[1] Margaret Gruca,[2] Mary A. Allen,[2] Vineela Kadiyala,[1] Tengyao Song,[1] Fabienne Gally,[3] Arnav Gupta,[4] Miles A. Pufall,[5] Robin D. Dowell,[2,6,7] and Anthony N. Gerber[1,3,4]

[1]*Department of Medicine, National Jewish Health, Denver, Colorado 80206, USA;* [2]*BioFrontiers Institute, University of Colorado, Boulder, Colorado 80309, USA;* [3]*Department of Biomedical Research, National Jewish Health, Denver, Colorado 80206, USA;* [4]*Department of Medicine, University of Colorado, Aurora, Colorado 80045, USA;* [5]*Department of Biochemistry, Carver College of Medicine, University of Iowa, Iowa City, Iowa 52242, USA;* [6]*Molecular, Cellular and Developmental Biology, University of Colorado, Boulder, Colorado 80309, USA;* [7]*Computer Science, University of Colorado, Boulder, Colorado 80309, USA*

The glucocorticoid receptor (NR3C1, also known as GR) binds to specific DNA sequences and directly induces transcription of anti-inflammatory genes that contribute to cytokine repression, frequently in cooperation with NF-kB. Whether inflammatory repression also occurs through local interactions between GR and inflammatory gene regulatory elements has been controversial. Here, using global run-on sequencing (GRO-seq) in human airway epithelial cells, we show that glucocorticoid signaling represses transcription within 10 min. Many repressed regulatory regions reside within "hyper-ChIPable" genomic regions that are subject to dynamic, yet nonspecific, interactions with some antibodies. When this artifact was accounted for, we determined that transcriptional repression does not require local GR occupancy. Instead, widespread transcriptional induction through canonical GR binding sites is associated with reciprocal repression of distal TNF-regulated enhancers through a chromatin-dependent process, as evidenced by chromatin accessibility and motif displacement analysis. Simultaneously, transcriptional induction of key anti-inflammatory effectors is decoupled from primary repression through cooperation between GR and NF-kB at a subset of regulatory regions. Thus, glucocorticoids exert bimodal restraints on inflammation characterized by rapid primary transcriptional repression without local GR occupancy and secondary anti-inflammatory effects resulting from transcriptional cooperation between GR and NF-kB.

[Supplemental material is available for this article.]

Glucocorticoids play a crucial role in normal physiology and are highly effective anti-inflammatory drugs with diverse clinical indications including asthma, rheumatoid arthritis, lupus, and inflammatory bowel disease, among many others (Morand 2000; Barnes 2006; Gerber 2015; Kim et al. 2017). Glucocorticoids exert their potent effects through binding to the glucocorticoid receptor (NR3C1, also known as the GR), which causes the GR to translocate to the nucleus and regulate gene expression through directly interacting with specific DNA sequences (Meijsing 2015; Sacta et al. 2016). Expression changes caused by glucocorticoids include gene induction and repression, with repression encompassing negative regulation of responses to inflammatory signals such as tumor necrosis factor (TNF) and lipopolysaccharide (LPS), including robust repression of cytokine expression (Rao et al. 2011; Uhlenhaut et al. 2013). Consequently, transcriptional repression is central to glucocorticoid-mediated anti-inflammatory effects (Clark and Belvisi 2012; Chinenov et al. 2013).

Pregenomics and deep sequencing-based approaches have established that inductive gene regulation by the GR is typically nucleated through protein-DNA interactions between homodimeric GR and high-affinity palindromic or semi-palindromic consensus GR binding sequences, which are found in regulatory regions of glucocorticoid-induced genes (La Baer and Yamamoto 1994; So et al. 2007; John et al. 2008). Mechanisms underpinning GR-mediated gene repression are less well understood. Although protein products resulting from GR-induced gene expression, such as TSC22D3 and DUSP1, are known to indirectly contribute to glucocorticoid-mediated transcriptional repression (Auphan et al. 1995; Ronchetti et al. 2015; Newton et al. 2017), direct repressive effects of the GR on inflammatory transcription factors, such as NF-kB, have long been viewed as principally responsible for the potent repressive effects of glucocorticoids on cytokine expression (Cruz-Topete and Cidlowski 2015; Vandewalle et al. 2018). Such primary repressive effects have been variably attributed to protein–protein tethering of the monomeric GR to DNA-associated inflammatory transcription factors, commonly referred to as transrepression (Ratman et al. 2013; De Bosscher et al. 2014), and also to protein-DNA interactions between the GR and so-called negative glucocorticoid response elements (nGREs) found within regulatory regions for inflammatory genes (King et al. 2013). Both mechanisms are purported to ultimately result in GR-centered

Corresponding author: gerbera@njhealth.org
Article published online before print. Article, supplemental material, and publication date are at http://www.genome.org/cgi/doi/10.1101/gr.248187.119.

recruitment of repressive complexes and down-regulation of specific inflammatory genes.

Controversy has emerged regarding putative repressive mechanisms. Enrichment for nGRE sequences within GR-occupied regions has not been evident on a genome-wide basis (Rao et al. 2011; Kadiyala et al. 2016; Oh et al. 2017). Similarly, repressive tethering interactions between the GR and NF-kB have not been uniformly observed in ChIP-seq studies (Uhlenhaut et al. 2013; Oh et al. 2017). Accordingly, the notion that GR-mediated repression is largely secondary, that is, a result of GR-induced targets exerting repressive effects, has recently been suggested (Cohen and Steger 2017; Oh et al. 2017). However, experiments with cycloheximide have indicated that protein synthesis is not required for at least partial glucocorticoid-based transcriptional repression (King et al. 2013). The structure of GR-nGRE complexes has also been described (Hudson et al. 2013), suggesting that such interactions could theoretically occur. Thus, there is ongoing debate regarding the fundamental mechanisms that underpin GR-mediated gene repression (Oh et al. 2017; Sacta et al. 2018). A definitive answer to this question would have crucial implications for understanding glucocorticoid-resistant inflammation and improving therapies.

To address this question, we previously used ChIP-seq to assess occupancy of GR, the RELA subunit of NF-kB, and RNA polymerase II (RNAPII) in BEAS-2B airway epithelial cells treated for 1 h with the potent synthetic glucocorticoid, dexamethasone (dex), TNF, and both dex and TNF (Kadiyala et al. 2016). Whereas our studies revealed rapid and robust reduction in RNAPII occupancy across a host of pro-inflammatory genes when cells were treated with dex + TNF versus TNF alone, our data did not confirm either a transrepressive or nGRE mechanism underlying these inhibitive effects on NF-kB. Instead, we discovered that GR and RELA cooperate through consensus binding sequences for both factors to enhance the expression of key anti-inflammatory genes, such as *TNFAIP3* (also known as A20). However, our studies lacked sufficient temporal resolution to determine whether GR-mediated repression is affected solely as a secondary consequence of inductive gene regulation, including targets of GR-RELA cooperation such as TNFAIP3, or whether primary repression of NF-kB activity by the GR also contributes to inflammatory repression by glucocorticoids.

Techniques that combine nuclear run-on approaches with deep sequencing (for example, global run-on sequencing or GRO-seq) are useful in defining enhancer activity and nascent transcriptional changes associated with signal transduction (Core et al. 2008; Hah et al. 2011; Allen et al. 2014). Thus, to address mechanisms through which glucocorticoids exert repressive effects on TNF signaling, we performed GRO-seq on BEAS-2B cells treated with dex, TNF, and dex + TNF for 10 or 30 min. Through integrating our GRO-seq results with ChIP-seq data and chromatin accessibility assays, we aimed to determine definitively whether the GR exerts classically described direct repressive effects on NF-kB or, instead, whether inflammatory repression can be fully attributed to other mechanisms.

Results

GRO-seq defines rapid effects of dex and TNF on gene transcription and identifies new anti-inflammatory targets of GR signaling

To determine mechanisms through which the GR represses gene expression, we performed GRO-seq on BEAS-2B airway epithelial cells treated for 10 and 30 min with vehicle (ethanol), TNF, dex, or TNF + dex. Differential transcription analysis (using an adjusted *P*-value $p_{adj} < 0.05$) of TNF or dex treatment alone relative to vehicle revealed that numerous genes show a robust transcriptional response after just 10 min (Fig. 1). At this early time point, the effects of TNF were exclusively inductive (Fig. 1A). Similarly, the majority (237 out of 259, or 95%) of loci regulated in response to 10 min of dex treatment were induced (Fig. 1B), although 12 genes (e.g., *KRT17*, Fig. 1B) exhibited statistically significant reduction in transcription. Given estimated rates of mammalian RNAPII transcription, mRNA maturation, and translation (Hargrove et al. 1991; Schwanhäusser et al. 2011; Cheng et al. 2016), both the 10- and 30-min time points are too rapid for protein synthesis from newly transcribed genes to occur. Supporting this notion, western blot analysis of TNFAIP3, NFKBIA, and CEBPB, all of which are transcriptionally induced by the GR (Supplemental File S1), did not demonstrate increases in protein expression after 30 min of dex treatment (Supplemental Fig. S1). Thus, the GRO-seq data are consistent with a direct repressive effect of ligand-activated GR on baseline RNAPII activity at specific genomic regions.

Comparison of the 10- and 30-min time points revealed that the genome-wide response is more pronounced at 30 min for both TNF and dex treatment, with 995 and 783 genes differentially transcribed, respectively (Fig. 1C,D; Supplemental File S1). Glucocorticoid-mediated repression was also more evident after 30 min of treatment, with 237 genes and long noncoding RNAs (lncRNAs) demonstrating reduced transcription (e.g., *MAFK*, Fig. 1D) based on $p_{adj} < 0.05$. Because of the more robust transcriptional response, we selected the 30-min time point for further analysis. Volcano plots of differentially regulated transcripts after 30 min of TNF versus TNF + dex treatment and dex versus TNF + dex treatment (Supplemental Fig. S2) indicate that both glucocorticoid and TNF signaling exert repressive effects on the other pathway. We subsequently further classified regulatory crosstalk between the two signaling pathways into three dominant clusters. In cluster one (Fig. 2A), comprising 117 genes, dex and TNF cooperated to enhance the transcription of target genes, a pattern linked to anti-inflammatory effects of glucocorticoids (Kadiyala et al. 2016). In cluster two (Fig. 2B), comprising 75 loci, dex repressed the transcription of TNF target genes, whereas reciprocally, TNF exerted a repressive effect on dex-mediated induction of 28 transcripts in cluster three (Fig. 2C). Supporting this transcription-based mechanistic organization, Gene Ontology analysis of differentially transcribed genes revealed a unique set of functional terms for each cluster (Supplemental Table S1).

Glucocorticoid signaling rapidly represses basal enhancer activity

Bidirectional transcription exclusive of gene transcription start sites, referred to herein as enhancer RNA (eRNA) transcription, can be used to characterize active enhancers (Allen et al. 2014; Azofeifa et al. 2018). We therefore used Transcription fit (Tfit), a machine learning program modeling RNAPII activity, to annotate putative eRNAs (Azofeifa and Dowell 2017). After merging putative eRNA regions across all samples, we obtained the set of active enhancers within this cell type ($n = 75{,}395$) and subsequently utilized DESeq2 (Love et al. 2014) to assess differential RNAPII activity in response to TNF, dex, or combinatorial treatment (Supplemental File S2). This analysis also allowed us to cluster differentially regulated enhancers into regulatory crosstalk patterns akin to those we had defined for gene transcription (Fig. 3A). Enhancers with activity patterns that mirrored the underlying regulatory pattern of the closest gene-encoding transcripts were

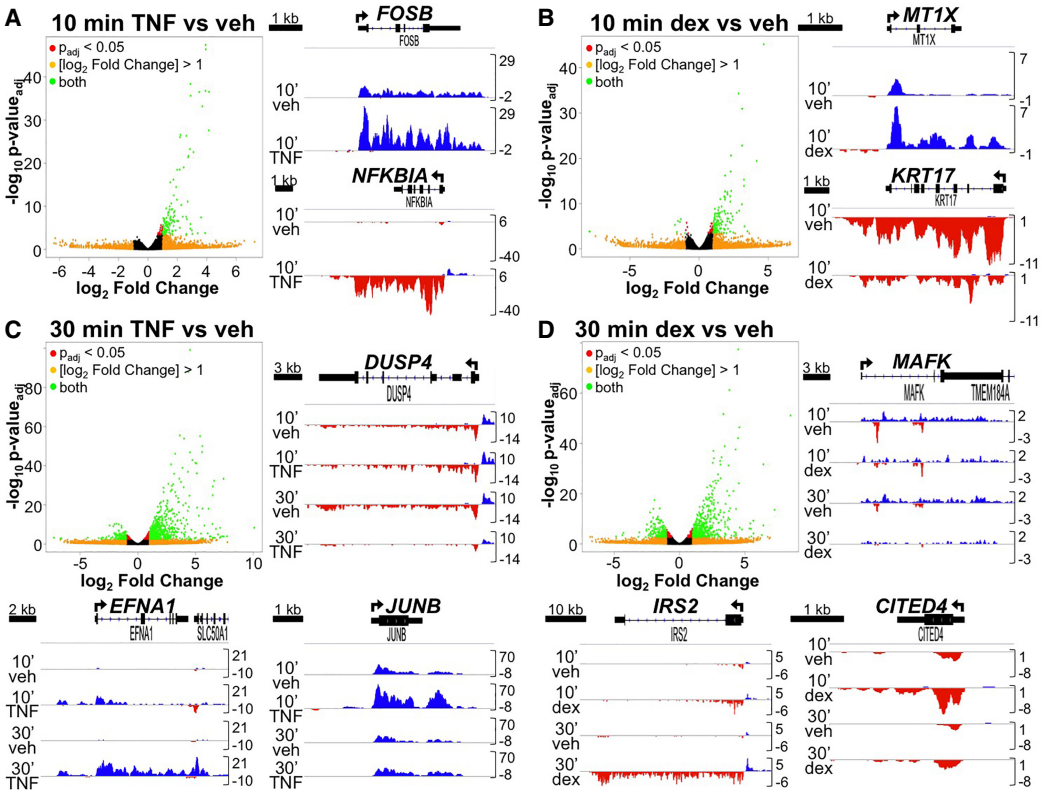

Figure 1. Primary transcriptional effects of TNF and glucocorticoids determined by GRO-seq. (*A–D*, *left*/*top*) Volcano plots indicating differentially regulated nascent transcripts in BEAS-2B cells treated with (*A*) 10 min TNF versus vehicle (veh), (*B*) 10 min dex versus veh, (*C*) 30 min TNF versus veh, and (*D*) 30 min dex versus veh. Representative examples are shown to the *right*/*bottom* of each volcano plot as GRO-seq tracks visualized in the Integrative Genomics Viewer (IGV) browser based on counts per million mapped reads (vertical scales). Positive (blue) peaks are reads annotated to the positive/sense strand while negative (red) peaks reflect reads annotated to the negative/antisense strand. The TSS and direction of transcription are indicated by arrows at the *top* of each screenshot.

readily identified within 39/117 cluster 1 transcripts, 23/75 cluster 2 transcripts, and 12/28 cluster 3 transcripts; average genomic distances between transcripts and the nearest enhancer in the same cluster are shown in Supplemental Figure S3.

Next, we scrutinized enhancers that exhibited reduced activity with TNF + dex treatment in comparison to TNF alone (analogous to cluster 2 in Fig. 2). Based on nonparametric testing, reduced enhancer activity with TNF + dex treatment versus TNF was strongly associated ($P < 0.00001$) with lower absolute levels of enhancer activity after dex treatment relative to vehicle (for examples, see Fig. 3, B and C). As NF-kB exhibits minimal basal occupancy in BEAS-2B cells (Kadiyala et al. 2016), these data do not support a singular mechanistic role for repressive tethering between the GR and NF-kB as the basis for dex-mediated repression of TNF signaling.

We were interested in determining whether enhancer activity defined by GRO-seq could, in an agnostic fashion, identify NF-kB and the GR as responsible for driving transcriptional effects of TNF and dex, respectively. To accomplish this, we used motif displacement (MD) analysis (Azofeifa et al. 2018), a metric that calculates the enrichment of transcription factor motifs within a 150-bp radius relative to motif frequency within a 1500-bp radius centered on Tfit-called enhancers. Comparing vehicle to TNF, the MD score for RELA (TF65) was the most increased across MD scores for all 641 transcription factors defined within the HOCOMOCO database (Supplemental Fig. S4; Kulakovskiy et al. 2018). There was no significant change in the MD score for the GR motif between vehicle and dex treatment. These data indicate that NF-kB binding sites are statistically enriched at the center of TNF-regulated enhancers, whereas regulation of enhancer transcription by the GR is less correlated with central enrichment for the consensus GR motif, as defined within the HOCOMOCO database.

ChIP-seq suggests glucocorticoids exert repressive effects on open chromatin without direct GR occupancy

To further assess primary repressive effects of dex on transcription, we analyzed dex-repressed enhancers in the context of our previously published ChIP-seq data (Kadiyala et al. 2016). Many of the dex-repressed enhancers exhibited presumptive GR binding peaks under basal culture conditions that were reduced with dex treatment (Supplemental Fig. S5), a phenomenon of unclear significance that we previously described (Kadiyala et al. 2016; Sasse et al. 2017). Possible explanations for these ChIP-seq peaks present at dex-repressed enhancers include a noncanonical interaction between the GR and chromatin in the absence of supplemental ligand, or alternatively, these peaks may result from nonspecific interactions between certain GR antibodies and so-called hyper-ChIPable genomic regions (Teytelman et al. 2013). To begin to distinguish between these possibilities, we performed western blots for GR protein on cytoplasmic and nuclear fractions of BEAS-2B cells. We did not detect nuclear GR in the absence of

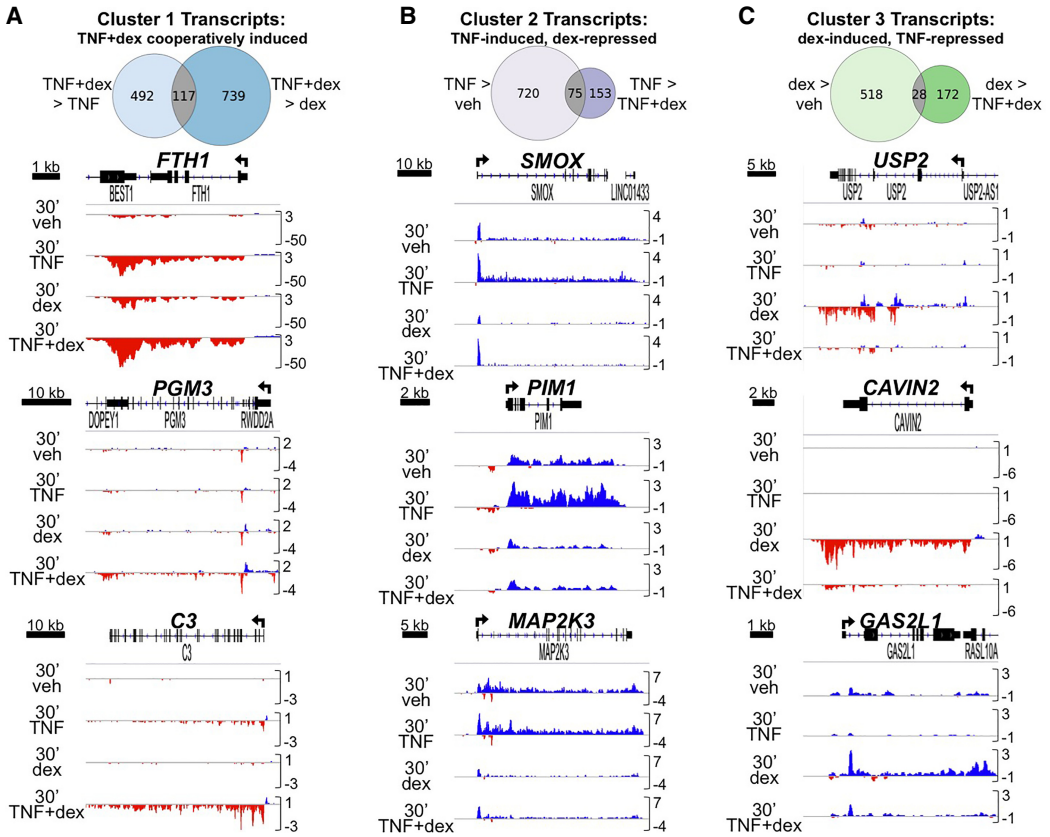

Figure 2. GRO-seq reveals distinct patterns of transcriptional crosstalk between TNF and dex. (*A–C, top*) Criteria used to cluster transcripts by indicated pattern of TNF + dex regulatory crosstalk and Venn diagrams showing how many differentially regulated transcripts (based on $p_{adj} < 0.05$) following 30-min treatment met the established criteria. (*A–C, bottom*) IGV screenshots of GRO-seq data, as described for Figure 1, illustrating examples of each crosstalk pattern.

dex (Supplemental Fig. S6), suggesting that GR ChIP-seq peaks seen in vehicle-treated cells with this antibody are artifacts. Moreover, many of the apparent GR binding peaks found under basal culture conditions overlap with open chromatin features (Tsompana and Buck 2014; Diehl and Boyle 2016; Castillo et al. 2017), including histone H3K27 acetylation and DNase I hypersensitivity, as observed in ENCODE data sets (see Supplemental Fig. S5). These data indicate that well-described nonspecific interactions between antibodies and open chromatin (Krebs et al. 2014; Jain et al. 2015) can confound analysis of GR occupancy at dex-repressed enhancers.

To address the propensity for ChIP artifacts at dex-repressed enhancer regions, we transduced cells with a lentiviral shRNA targeting GR (shGR) or a control (shCtrl). Pilot qRT-PCR assays confirmed that the effects of dex on gene expression were significantly reduced in shGR cells (Supplemental Fig. S7). We used the shGR system to perform ChIP-seq experiments with two different antibodies: GR-lA1, which previously showed significant peaks under basal culture conditions, and a new antibody, GR-356, which showed minimal basal occupancy in pilot experiments. Both antibodies were generated against the same GR epitope and recognize a single appropriately sized protein that is reduced in shGR cells (Supplemental Fig. S8). To align with our prior ChIP-seq studies, shGR and shCtrl BEAS-2B cells were treated for 1 h with vehicle, TNF, dex, or TNF + dex. Initial analysis of both the GR-IA1 and GR-356 ChIP-seq data sets revealed that canonical sites of GR occupancy exhibited dex-inducible ChIP-seq peaks that were abrogated in shGR cells (Fig. 4A). We subsequently assessed these data on a genome-wide basis through MD analysis. When applying the MD score approach to ChIP-seq data, we centered on MACS2-called ChIP-seq peaks within data sets for each condition. This revealed highly significant central enrichment for the canonical dimeric GR binding motif in shCtrl cells treated with dex (MD scores of 0.43 and 0.67 with GR-lA1 and GR-356, respectively). Consistent with ~90% GR knockdown achieved in cells transduced with shGR (Supplemental Fig. S8), enrichment for the GR motif was significantly abrogated ($P < 0.00005$), but not wholly eliminated, in ChIP-seq data from shGR cells (Fig. 4B; Supplemental Fig. S9). In contrast, MD scores for two potential matches to the so-called nGRE motif ranged from 0.13 to 0.15. These scores are similar to the expected score of 0.1 for a randomly distributed motif. Moreover, these scores were not significantly altered in cells transduced with shGR (Fig. 4B; Supplemental Fig. S10), rendering it unlikely that the GR interacts specifically with these nGRE sequences.

Unlike the concordant results from both antibodies indicative of GR occupancy at canonical binding sites, ChIP-seq patterns in vehicle- and TNF-treated cells showed substantial differences between the two antibodies. For the GR-lA1 antibody, MACS2-identified peaks were observed in basal culture conditions ($n = 68,278$ peaks), including at TNF-induced enhancers (Fig. 4C), in association with highly significant MD scores for AP-1 family members

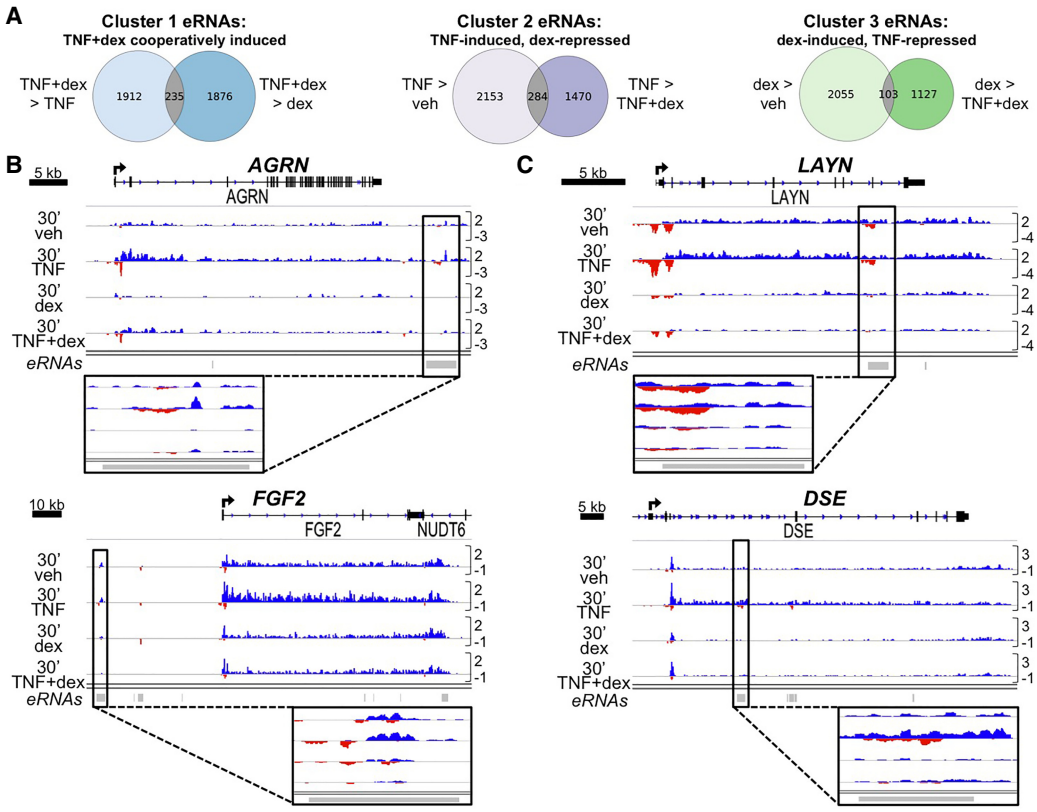

Figure 3. Glucocorticoids promptly repress basal activity of TNF-induced enhancers defined by bidirectional GRO-seq signature. (*A*) Criteria used to cluster bidirectional enhancer signatures by TNF + dex crosstalk pattern and Venn diagrams illustrating the number of differentially transcribed eRNAs (using nonadjusted *P*-value < 0.05) meeting these criteria. (*B*,*C*) IGV-visualized GRO-seq tracks of cluster 2 (TNF-induced, dex-repressed) transcripts and nearby (*B*) intergenic or (*C*) intragenic called eRNAs (signified by gray bars at the *bottom* of each screenshot) exhibiting a similar regulatory pattern.

(Fig. 4D). Minimal enrichment for canonical NF-kB binding motifs was also detected, which was significantly increased with TNF treatment (Fig. 4D). MD scores for the AP-1 family and the NF-kB complex were not significantly reduced in shGR cells (Supplemental Figs. S9, S10). Taken together, given the lack of nuclear GR (Supplemental Fig. S6) and the failure of stable GR knockdown to consistently reduce the MD scores for AP-1 family and NF-kB complex motifs, these data indicate that the GR-lA1 ChIP-seq peaks present in vehicle- and TNF-treated cells do not represent bona fide interactions between the GR protein and chromatin. Instead they reflect nonspecific interactions between this GR antibody and hyper-ChIPable genomic regions.

In contrast to the GR-lA1 antibody, the GR-356 ChIP-seq data showed minimal detectable MACS2-identified peaks with vehicle and TNF treatment ($n = 251$ and 271 peaks, respectively) (e.g., Fig. 4C), suggesting that this antibody is less prone to artifactual interactions. Thus, to determine whether local GR occupancy is required for repression of TNF-regulated enhancers, we integrated the GRO-seq and GR-356 data with our published ChIP-seq analysis of RELA occupancy (Kadiyala et al. 2016). Enhancers with TNF-inducible RELA occupancy that were repressed by dex without detectable GR occupancy were readily identified (Fig. 4E). Indeed, out of a total of 252 enhancers that exhibited dex-mediated repression, 119 had no evidence of GR occupancy. Thus, within the limits of our ChIP-seq assays, tethering interactions between GR and NF-kB and/or direct occupancy of GR at specific enhancers are not required for dex-mediated repression. We also failed to detect evidence of tethering at several GR-repressed targets using ChIP-qPCR (Supplemental Fig. S11).

To explore further whether our data provide evidence of repressive tethering between the GR and other transcription factors, we performed MD analysis. MD scores ranged between 0.14 and 0.17 for NFKB1 and RELA binding motifs within the dex-treated GR-356 ChIP-seq data set (Fig. 4F), indicative of only minimal central enrichment for NF-kB complex binding sequences. Moreover, the MD scores for NFKB1 and RELA are lower than MD scores for motifs associated with numerous other transcription factor families, including AP-1 (top score 0.46), BACH (top score 0.31), RUNX (top score 0.29), NFI (top score 0.28), and TEAD (top score 0.24) families, among others (Supplemental Fig. S10; the entire set of MD scores is available in Supplemental File S3). These data are consistent with well-described combinatorial transcriptional regulation by the GR and other transcription factors through canonical binding sites (Wang et al. 1999), rather than a protein-tethering regime that would encompass interactions between the GR and such widely diverse transcription factors.

Integrated analysis of dex-repressed enhancers

The GR has been reported to exhibit dynamic genomic occupancy that is detectable at some sites within 10 min of glucocorticoid exposure. Thus, to determine whether the GR transiently occupies a larger fraction of dex-repressed enhancers than we detected after 1 h of dex treatment, we performed ChIP-seq using the GR-356

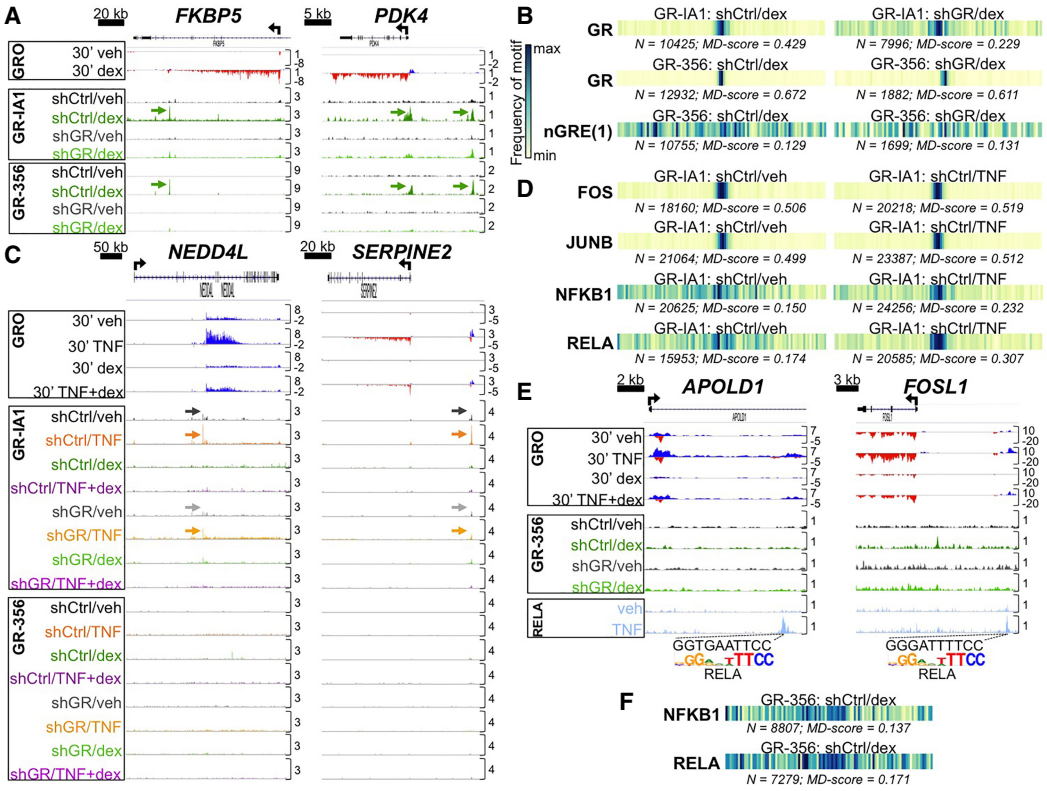

Figure 4. GR ChIP-seq with stable GR knockdown establishes that direct enhancer occupancy by the GR is not required for primary glucocorticoid repression of TNF targets. (*A*) Aligned GRO-seq and GR ChIP-seq IGV tracks at representative dex-induced loci; arrows indicate GR peaks associated with canonical GR binding sites. Vertical scales indicate maximum counts per million mapped. (*B*) Motif displacement (MD) analysis depicting frequency of sequence overlap with a GR and a representative nGRE binding motif within ±1500 bp of GR ChIP-seq peak summits in the indicated data sets. Each column of the barcodes is a bin of a histogram (100 bins total) where heat is proportional to the frequency of the motif instance at that distance from a ChIP-seq peak center. Darker colors signify greater enrichment on a 0–1 scale. (*C*) ChIP-seq and GRO-seq IGV tracks at dex-repressed loci exhibiting apparent GR occupancy in veh- and TNF-treated shCtrl cells (indicated by arrows) with the GR-IA1 but not the GR-356 antibody. (*D*) MD analysis of enrichment for NF-kB complex and AP-1 family motifs in the indicated ChIP-seq data sets. (*E*) GR-356 ChIP-seq (and GRO-seq) data combined with RELA ChIP-seq tracks (Kadiyala et al. 2016), illustrating dex-mediated repression of RELA-occupied enhancers containing NF-kB/RELA binding motifs in the absence of GR occupancy. (*F*) MD analysis for NF-kB complex motifs in the indicated ChIP-seq data sets.

antibody on cells treated with dex for 10 min. MD analysis performed using an expanded database of TFs to potentially define new interacting sites (Lambert et al. 2018) revealed a highly significant GR motif score (Fig. 5A). We next overlapped 10-min MACS2-defined GR peaks (Supplemental File S4) with enhancers that showed increases or decreases in activity based on the 30-min GRO-seq data ($p_{adj} < 0.05$). This showed that approximately half (384/759) of dex-induced enhancers are associated with GR binding peaks after 10 min of dex treatment, whereas <10% (23/252) of dex-repressed enhancers show detectable peaks (Fig. 5B). Examples of GR-mediated transcriptional induction associated with GR occupancy and repression without evidence of GR occupancy after 10 min of dex are shown in Fig. 5C.

Although collectively, at the level of resolution afforded by our ChIP-seq assays, our data indicate that GR occupancy is not a requirement for dex-mediated repression of enhancer activity, we were interested in further exploring the set of dex-repressed enhancers with dex-induced GR-356 peaks. When we visualized the aggregate ChIP- and GRO-seq data for such genomic regions in comparison to regions with dex-induced enhancer activity, we observed qualitative differences in occupancy patterns. As shown in Figure 5D, dex-induced peaks associated with a typical dex-induced enhancer (in this case, 5′ of *BIRC3*) exhibited maximal occupancy with dex treatment in the ChIP-seq data for both the GR-IA1 and GR-356 antibodies that was reduced substantially in shGR cells across conditions. In contrast, the detectable peaks resulting from ChIP with the GR antibodies at dex-repressed enhancers, exemplified here by the *MYEOV* locus, were significantly more variable. Specifically, large GR-IA1 vehicle peaks were detected at these sites, whose magnitude largely mirrored the magnitude of the peaks detected with the GR-356 antibody after dex treatment (cf. peaks in GR-IA1 shCtrl/veh to GR-356 shCtrl/dex in *MYEOV* panel, Fig. 5D). Moreover, the reduction in peak size comparing ChIP-seq data from shGR to shCtrl cells at canonical dex-induced sites was significantly greater than at dex-repressed enhancers. For example, the magnitude of the shGR/TNF + dex peaks within the *MYEOV* locus was greater than the shCtrl/TNF + dex peaks, a finding that is inconsistent with these peaks representing bona fide GR occupancy, especially since the opposite pattern was observed at canonical dex-induced enhancers. This paradoxical finding was reiterated at other genomic sites of repression (see Supplemental Fig. S12). In total, 23/133 dex-repressed enhancers with dex-induced peaks in the GR-356 shCtrl ChIP-seq data also had peaks in the same location in the GR-356 shGR/TNF + dex ChIP-seq data. Further quantification of characteristics of the dex-repressed enhancers harboring dex-induced GR binding peaks with the

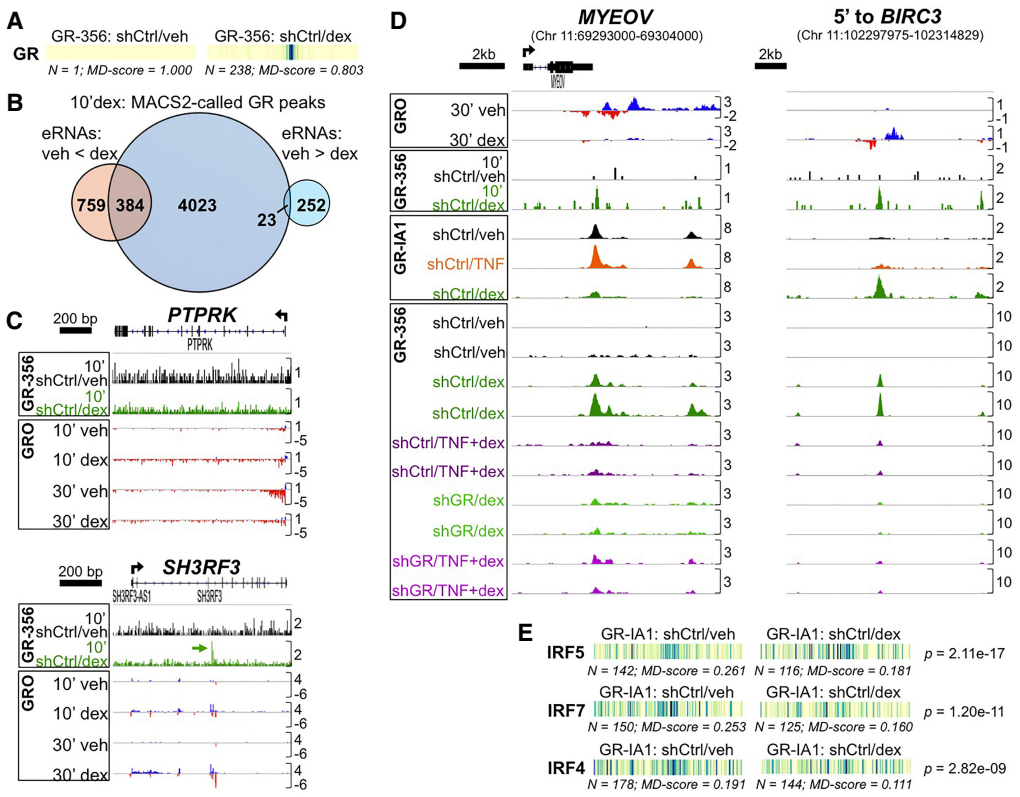

Figure 5. Integrated analysis of 10-min and 1-h GR ChIP-seq data with enhancer activity defined by GRO-seq. (*A*) Motif displacement analysis of 10-min GR ChIP-seq data reveals robust central enrichment of the GR binding motif. (*B*) Venn diagram indicating ~50% overlap between 10-min dex-induced GR binding peaks and dex-induced enhancers versus <10% overlap with repressed enhancers. (*C*) Example of a dex-repressed enhancer (*PTPRK*) with no 10-min GR peaks and a dex-induced enhancer (*SH3RF3*) with a dex-induced peak after 10 min. (*D*) Integrated ChIP- and GRO-seq analysis reveals qualitatively different occupancy patterns between GR-repressed (*MYEOV*) and GR-induced (5′ to *BIRC3*) enhancers. (*E*) Motif displacement analysis applied to GR-IA1 vehicle versus dex ChIP-seq data.

GR-356 antibody revealed that more than 90% of these peaks overlapped with peaks from the GR-IA1 vehicle ChIP-seq data set. Moreover, out of the entire set of 252 dex-repressed enhancers, 194 were in hyper-ChIPable regions based on colocalization of a GR-IA1 vehicle peak. Taken together, although we observed dex-induced occupancy in the GR-356 ChIP-seq data set at ~50% of dex-repressed enhancers, integrated analysis of our entire set of ChIP-seq data indicates these peaks are likely influenced by underlying hyper-ChIPable characteristics of dex-repressed enhancer regions.

Given the significant overlap between GR-IA1 vehicle peaks and repressed enhancers, we further analyzed the GR-IA1 ChIP-seq data in relationship to dex-induced, dex-repressed, and "no significant change" enhancers. We observed statistically significant reductions in peak magnitude at repressed enhancers comparing vehicle to dex treatment only in shCtrl cells (Supplemental Fig. S13; Supplemental Table S2). We therefore applied MD analysis to the GR-IA1 vehicle versus dex peaks from shCtrl cells using the human transcription factor catalog (Lambert et al. 2018). We found highly significant decreases in MD scores for several IRF family transcription factors (Fig. 5E; Supplemental File S5). In contrast, based on aligning Tfit-called enhancers with H3K27 acetylation data generated by the ENCODE consortium from other cell types (Davis et al. 2018), specific basal histone H3K27 acetylation levels do not appear to predict enhancer responses to dex on a genome-wide basis (Supplemental Figs. S14, S15).

Glucocorticoids cause rapid changes in chromatin accessibility

The changes we observed in nonspecific interactions between the GR-IA1 antibody and chromatin, as evidenced by significant changes in MD scores for multiple factors (Figs. 4D, 5E; Supplemental Fig. S9), suggest that dex treatment directly modifies the chromatin structure of these enhancers. The GR has been previously reported to modify chromatin structure (John et al. 2008; Oh et al. 2017), although the contextual resolution of enhancer activity provided by GRO-seq was not available in those studies. We therefore performed high-resolution micrococcal nuclease (MNase) accessibility assays in BEAS-2B cells treated with vehicle or dex for 10, 30, or 60 min. Using tiled qPCR, we imputed relative protection from MNase digestion, a reflection of chromatin accessibility (Infante et al. 2012), across ~700–1500 bp of representative dex-repressed and dex-induced enhancers. These data show a rapid increase in protection from MNase digestion within part of each GR-repressed enhancer (*PTPRK* and *TMEM217* in Fig. 6A,B; *SMURF2* in Supplemental Fig. S16); these enhancers did not exhibit significant occupancy with the GR-356 antibody under any treatment condition (Supplemental Fig. S17). In contrast, protection from MNase cleavage was reduced within the two dex-induced enhancers tested with this assay (*ANGPTL4* and *SH3RF3* in Fig. 6C,D), and these enhancers showed significant dex-induced GR occupancy (Supplemental Fig. S17). For each of our interrogated enhancers, the flanks were protected from digestion, consistent

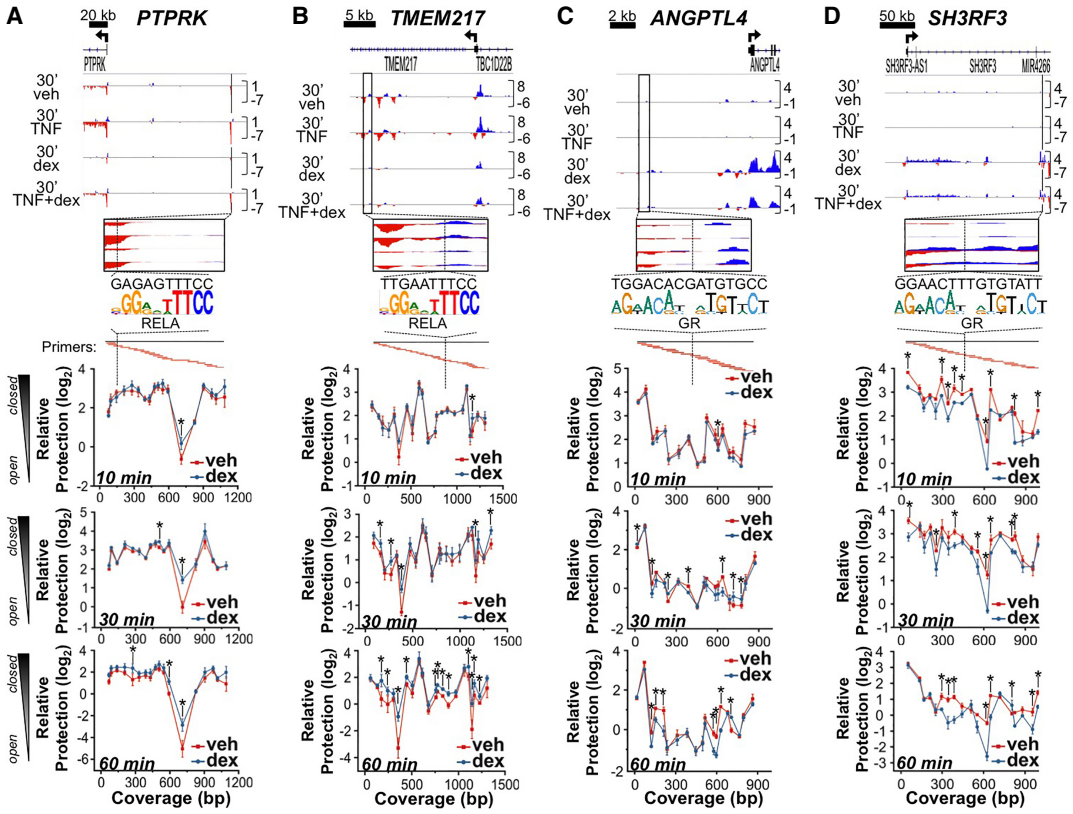

Figure 6. Dex treatment rapidly changes basal chromatin structure of both TNF- and dex-induced enhancers. (*A–D*, *top*) IGV screenshots of GRO-seq data with solid black lines/rectangles showing specific TNF-induced (*A,B*) and dex-induced (*C,D*) enhancer regions that were interrogated by the MNase assay. *Below* each screenshot is a zoomed-in view of each assayed region, including the location (dotted black line) and sequence of the strongest match to the NFKB(1,2)/RELA consensus binding motif (*A,B*) and GR binding motif (*C,D*). *Beneath* the binding site matches are the locations of overlapping tiled qPCR primers (amplicons in red) that span each region and correspond to the data points in the line graphs *below*. (*A–D*, *bottom*) Mean relative protection (±SD) against MNase cleavage of each target region as measured by qPCR in BEAS-2B cells treated with veh or dex for 10, 30, or 60 min. (*) $P < 0.05$ versus veh with Bonferroni correction. Greater protection indicates less accessibility or a more closed chromatin structure, as illustrated on the far *left*.

with positioned nucleosomes flanking these regulatory elements. Thus, rapid internucleosomal changes in enhancer chromatin structure can occur with dex treatment, characterized by decreased access to MNase digestion at dex-repressed enhancers and increased access to MNase digestion at dex-induced enhancers. Moreover, reporter analysis using a short half-life luciferase system (Masser et al. 2016) showed that enhancers from cluster 1 (i.e., cooperative regulation by TNF and dex) mimicked the behavior of the endogenous enhancer (Supplemental Fig. S18). In contrast, repressive effects of dex on cluster 2 enhancers in reporter assays were not evident at the 1-h time point and were not detected until 4 h for *IER3*. Thus, rapid repressive effects of dex on enhancer activity appear to depend in part on genomic context, providing further support for a chromatin-based primary repressive mechanism.

Discussion

In this study, we set out to determine whether glucocorticoids exert primary repressive effects on gene expression, defined as repression occurring without a protein intermediate. Our GRO-seq data, which show reduced nascent transcription in some genomic regions after just 10 min of dex treatment, provide strong evidence in support of direct repressive effects. Repression of many TNF-regulated enhancers and genes occurred in the absence of TNF treatment, indicating, as suggested by others (Jubb et al. 2016; Oh et al. 2017), that tethering between the GR and RELA is not required for a primary response. Moreover, the previously described nGRE sequence was not significantly enriched within GR occupied regions, indicating that widespread repression does not occur through direct interactions between the GR and nGREs in our system. Instead, our analysis of GR ChIP-seq data with and without stable GR knockdown suggests that many dex-repressed enhancers reside in so-called hyper-ChIPable regions of the genome that are subject to nonspecific interactions with antibodies in ChIP assays. Dynamic changes in these nonspecific interactions between GR antibodies and enhancer chromatin with dex and TNF treatment, in conjunction with MNase accessibility assays of representative enhancers, indicate that dex treatment rapidly changes the chromatin structure at repressed enhancers in a process that does not require GR occupancy. Taken together, our data establish that glucocorticoids exert primary repressive effects on transcription through altering chromatin structure. However, the two dominant explanations for primary repression, GR tethering to NF-kB and interactions between the GR and nGREs, are unable to account for these effects on a genome-wide basis.

What is the mechanistic basis for primary GR-mediated repression? Although we cannot entirely rule out nonartifactual direct interactions between the GR and chromatin as a cause of reduced enhancer activity at a subset of repressed enhancers, our data clearly indicate that there is no universal requirement for

such occupancy. Instead, our data support a model in which dex-induced genome-wide binding of the GR to canonical binding sites results in reciprocal, repressive alteration of chromatin structure at selected enhancers that are not directly occupied by the GR (Fig. 7). Although speculative, this could occur through a variety of mechanisms including allosteric or biophysical effects of GR-nucleated transcription complexes on chromatin topology, three-dimensional interactions between the GR and the repressed enhancers, and/or context-dependent redistribution of coregulators that are required to maintain open chromatin structure at the dex-repressed enhancers. Whether primary repression in association with chromatin tightening is a property of physiologic nuclear receptor signaling also remains to be determined. In that regard, we speculate that normal circadian pulses of corticosteroids, which are known to reduce cytokine expression (Gibbs et al. 2014), may restore "chromostasis" or a neutral chromatin structure in cells that have experienced activation of inflammatory genes during the course of the preceding 24 h. In this scenario, active inflammatory signaling that culminates in transcription factors interacting with primary dex-repressed enhancers could both counteract physiologic return to chromostasis and also reduce the effectiveness of glucocorticoid-based medications. In an extension of this notion, our finding that IRF family binding sequences are located within chromatin regions subject to dex-mediated repression (Fig. 5E) provides a potential explanation for recently reported associations between elevated interferon levels and severe, glucocorticoid-resistant asthma (Raundhal et al. 2015).

Our finding that many GR-repressed enhancers, as definitively established by GRO-seq, are in genomic regions with hyper-ChIPable characteristics is significant in light of the ongoing dissonance in the literature related to GR-mediated repression. In some recent publications, the premise that the GR exerts transrepressive effects to repress inflammation is asserted as established fact (Hua et al. 2019). In contrast, other studies have questioned the mechanistic importance of transrepression but nevertheless reported small dex-induced peaks in GR ChIP-seq data at presumptive repressed enhancers (Oh et al. 2017; McDowell et al. 2018). The significance of these peaks, which are very similar to the GR-356 antibody peaks we observed within hyper-ChIPable regions at ~50% of repressed enhancers, was not determined. Widespread monomeric GR genomic occupancy in vivo under basal physiologic conditions has also been reported. Glucocorticoid treatment decreased occupancy at these basal peaks with concomitant increased GR occupancy at canonical dimeric sites, and transcriptional repression occurred at genes linked to the basal GR peaks (Lim et al. 2015). Here, too, the pattern is strikingly similar to the dynamic artifactual occupancy pattern we observed at dex-repressed enhancers, in this case with the GR-IA1 antibody in vehicle versus dex-treated cells. Although we have not specifically investigated whether these and other published GR ChIP-seq data sets are confounded by nonspecific interactions between antibodies and chromatin, dynamic hyper-ChIPable properties of dex-repressed enhancers that we have characterized here could potentially influence a range of experimental systems, thus providing parsimony for seemingly discordant data.

It has been argued that redistribution of limiting amounts of specific coregulators from one set of enhancers to another is a unifying explanation for rapid repression in association with transcriptional induction (Guertin et al. 2014; Schmidt et al. 2016), which has been observed in a variety of other signaling contexts (Hah et al. 2011; Step et al. 2014; Franco et al. 2015; Loft et al. 2015; Toropainen et al. 2016). Several groups have specifically reported on glucocorticoid-induced genomic redistribution of transcription factors and cofactors (Swinstead et al. 2016; McDowell et al. 2018). However, our data suggest that a simple titration model of general co-activators, such as EP300, is unlikely to fully explain primary repression. Indeed, whereas genomic EP300 occupancy is extensive and broadly associated with active enhancers (Visel et al. 2009), we found that tens of thousands of active enhancers were not significantly repressed by dex. Furthermore, conclusions regarding putative transcription factor redistribution need to specifically account for the hyper-ChIPable nature of regulatory regions that are subject to the rapid repressive and chromatin remodeling effects of glucocorticoids. Whereas numerous studies have reported on chromatin structure remodeling in association with GR signaling (John et al. 2008; Voss et al. 2011; Jubb et al. 2017; McDowell et al. 2018), our MNase data indicate that remodeling at some sites is associated with changes in

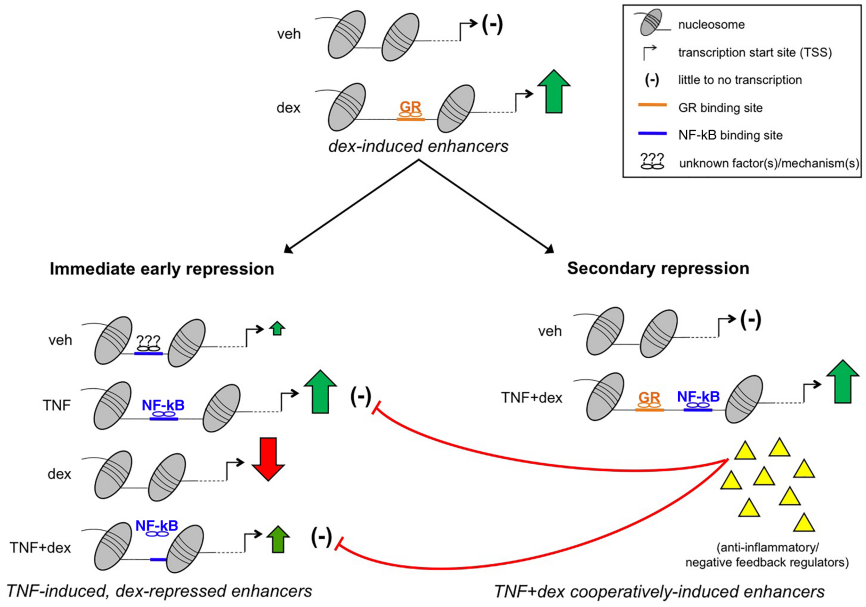

Figure 7. Two-step model of glucocorticoid-mediated inflammatory repression. Glucocorticoids rapidly induce target genes predominantly through glucocorticoid receptor (GR) interactions with enhancers harboring canonical GR binding sites (GBSs). The consequences of genome-wide transcriptional induction by the GR include (1) an immediate early wave of repression, characterized by rapid reciprocal internucleosomal tightening at select TNF-induced enhancers that is independent of local GR occupancy, and (2) a secondary wave of repression resulting from downstream effects of genes induced by specialized enhancers subject to cooperative regulation by GR and NF-kB. These cooperatively regulated secondary effectors exert robust negative feedback control to limit further NF-kB activity and also function to counteract/destroy the various pro-inflammatory products (e.g., cytokines, chemokines, proteases) generated during the initial response, thereby playing a crucial role in promoting complete resolution of inflammation.

internucleosomal accessibility (e.g., *PTPRK*) (Fig. 6A) rather than broad changes in nucleosome positioning. These changes in internucleosomal access may lead to dynamic alterations in nonspecific interactions between antibodies and these chromatin regions being observed in ChIP-seq data sets. Chromatin structure changes could also influence the efficiency of even bona fide antibody-transcription factor interactions with chromatin, thus creating potential for further bias in strategies that equate read number at specific genomic regions across different ChIP-seq data sets with actual occupancy of the factor of interest.

In addition to demonstrating that glucocorticoid signaling exerts primary repressive effects on transcription, our GRO-seq data build on prior work implicating cooperative glucocorticoid-TNF crosstalk in secondary repression of inflammatory processes (Vettorazzi et al. 2015; Kadiyala et al. 2016). Specifically, the high resolution afforded by GRO-seq allowed us to discover additional target genes in which dex + TNF treatment resulted in higher levels of RNAPII activity than was evident with dex or TNF alone. Novel targets of glucocorticoid-TNF cooperation include *PGM3*, whose deficiency is associated with elevated IgE levels and asthma (Yang et al. 2014), *FTH1*, which protects against TNF-mediated apoptosis (Pham et al. 2004), and *C3*, a traditionally pro-inflammatory gene that was recently reported to suppress stress-associated apoptosis in BEAS-2B airway epithelial cells (Kulkarni et al. 2019). The anti-inflammatory functions of each of these genes further implicate cooperative gene regulation by the GR and NF-kB as an important mechanistic underpinning of repression of inflammation and cell injury by glucocorticoids.

A number of classically inductive signaling pathways, including estrogen signaling, exert primary repressive effects on transcription that encompass repression of TNF target genes (Ruan et al. 2003; Franco et al. 2015). The estrogen receptor can also cooperate with NF-kB to induce gene expression (Franco et al. 2015). Why then do glucocorticoids function as uniquely potent anti-inflammatory drugs? The data we have presented here, in combination with prior work reporting on cooperative anti-inflammatory gene regulation by the GR and NF-kB (Altonsy et al. 2014; Vettorazzi et al. 2015; Sasse et al. 2016), provide insight into this unmatched clinical efficacy. Specifically, our data support a two-step model (see Fig. 7) in which inductive gene regulation by GR results in rapid reciprocal repression of inflammatory enhancers through a chromatin-based repressive mechanism. Whereas this form of reciprocal repression is not exclusive to glucocorticoids, through canonical binding sites for the GR and NF-kB, the activity of a subset of specialized enhancers controlling anti-inflammatory genes is uniquely augmented by glucocorticoids in cooperation with NF-kB. This GR-specific regulatory system renders these anti-inflammatory genes relatively resistant to both primary repression and to negative feedback control of NF-kB, thus decoupling the expression and resulting biologic effects of these negative feedback regulators from pro-inflammatory cytokine expression. With respect to the airway, the targets we have found that are regulated through this cooperative mechanism encompass a range of genes that protect against various forms of cellular stress, as well as several powerful negative feedback regulators of NF-kB, including TNFAIP3. Our data thus provide an explanation for the clinical effectiveness of glucocorticoids in reversing inflammation associated with asthma and chronic obstructive pulmonary disease exacerbations, which are typically a consequence of airway infections that both induce NF-kB signaling and cause cellular injury (Kersul et al. 2011; Hoppenot et al. 2015; Nicod and Kolls 2015; Schuliga 2015). Our findings may also enable rational pharmacologic improvement of glucocorticoid-mediated inflammatory repression, a long-sought goal in pulmonary therapeutics (Barnes 2006; Clark and Belvisi 2012).

Methods

Cell culture, reagents, western blotting, and qPCR

Cell culture and western blotting were performed according to standard protocols with reagents as detailed in the Supplemental Methods. For lentiviral production, HEK293 FT cells were grown to ~70% confluence on Poly-D-Lysine-coated 10-cm tissue culture dishes and transfected with lentiviral packaging vectors pMDLG/RRE, pMD2.G, and pRSV/Rev (2.88 µg total, Addgene) plus pMK1221-control or -GR shRNA (2.88 µg shCtrl or shGR, respectively) using TransIT-293 Transfection Reagent (Mirus Bio). The shGR construct was cloned as described (Kampmann et al. 2014) and targeted the following sequence: TGGTGTCACTGTTGGAG GTTAT. qPCR was performed as described (Sasse et al. 2013). Primer sequences are in Supplemental Tables S4 and S5.

Global run-on sequencing and analysis

Our GRO-seq protocol was based on previous publications (Allen et al. 2014), as detailed in the Supplemental Methods.

Data processing, visualization, and identification of eRNAs

Two biological replicates of each treatment (veh, TNF, dex, and TNF + dex) at both 10- and 30-min timepoints were processed using an nf-core nascent Nextflow pipeline (https://github.com/nf-core/nascent; DOI: 10.17605/OSF.IO/NDHJ2). A full pipeline report of the run as well as a quality control report generated by MultiQC (v. 1.7) (Ewels et al. 2016), including trimming, mapping, coverage, and complexity metrics, are included in Supplemental File S6. Normalized TDF coverage files output by the pipeline were visualized using the Integrative Genomics Viewer (IGV, v. 2.4.10) (Robinson et al. 2011). Application of FStitch and Tfit to identify regions with bidirectional transcriptional activity is detailed in the Supplemental Methods and output files are included in Supplemental File S7.

Differential transcription analysis of genes and bidirectionals/eRNAs

Using the RefSeq:NCBI Reference Sequences for hg38, including both NM and NR accession types (downloaded from the UCSC track browser on May 18, 2018), counts were calculated for each sorted BAM file using multiBamCov in the BEDTools suite (v. 2.25.0) (Quinlan and Hall 2010). Genes (NM accession type) and lncRNAs (NR accession type) were then filtered such that only the isoform with the highest number of reads per annotated length was kept in order to minimize duplicate samples being included in differential transcription analysis. DESeq2 (v. 1.20.0, Bioconductor release v. 3.7) was then used to determine which genes were differentially transcribed between the different treatments for each time point separately (Supplemental File S1). For bidirectional/eRNA comparisons, all bidirectional prediction Tfit calls were first merged using mergeBed (argument -d 60) from the BEDTools suite (v. 2.25.0) to generate an annotation file. Counts were then calculated for each sample using multicov from the BEDTools suite (v. 2.25.0), and DESeq2 was used to calculate differentially transcribed bidirectionals/eRNA (Supplemental File S2). Scripts and data processing information are available at https://github.com/Dowell-Lab/Sasse2019 and in the Supplemental Code.

Chromatin immunoprecipitation-sequencing (ChIP-seq)

For the 1-h ChIP-seq experiment, BEAS-2B cells transduced with lentiviral shCtrl or shGR were grown to confluence in 10-cm tissue culture dishes ($\sim 10 \times 10^6$ cells/plate). Cells were crosslinked by adding 16% methanol-free formaldehyde to a final concentration of 1% and incubating for 5 min at room temperature. ChIP was then performed as described (Sasse et al. 2013), with the exception that samples were sonicated (Diagenode Bioruptor) on high power for 35 cycles of 30-sec bursts separated by 30-sec incubations in ice water. Samples were immunoprecipitated with 12 µg of GR-356 or GR-IA1 antibody. One nanogram of purified ChIP (or Input) DNA was used to prepare uniquely barcoded libraries with the Ovation Ultralow Library System from NuGEN. Libraries were pooled and sequenced in duplicate on an Illumina NovaSeq using 2 × 150-bp paired-end reads. For the 10-min experiment, shCtrl-transduced BEAS-2B cells were treated with vehicle or dex and processed for ChIP using 12 µg of GR-356 antibody. ChIP and Input DNA libraries were prepared with a KAPA HyperPrep kit and sequenced in duplicate on an Illumina NextSeq using a V2 High Output 1 × 75-cycle single-end kit. Computational details are in the Supplemental Methods. MultiQC reports for ChIP-seq are in Supplemental Files S8 and S9. MACS2 (Zhang et al. 2008) analysis for 1-h ChIP-seq is in Supplemental File S10.

Motif displacement analysis

Tfit-called bidirectionals/eRNAs or MACS2-called ChIP-seq peaks were used as input for DAStk (v. 0.1.5; https://github.com/Dowell-Lab/dastk) to calculate motif displacement scores (Tripodi et al. 2018), which quantify the degree of colocalization of transcription factor consensus binding motifs with the center of each eRNA origin or ChIP-seq peak. FIMO (Grant et al. 2011) was used to identify matches to consensus binding motifs using a *P*-value cutoff of 10^{-5} with arguments "-max-stored-scores 10,000,000 -thresh 1×10^{-5}" as defined by the 641 binding motif position weight matrices (PWMs) obtained from the HOCOMOCO database (v. 11) and/or an expanded set of PWMs obtained from a curated human transcription factor database (Kulakovskiy et al. 2018; Lambert et al. 2018). To generate barcode plots, consensus binding motifs were mapped to hg38 using a *P*-value cutoff of 10^{-5}. For each motif instance, the number of hits using the ChIP-seq peak or Tfit-called bidirectional/eRNA center was used to calculate motif displacement in a 3000-bp window around the center of the feature. A *z*-test of two proportions was used to determine statistically significant differences in the calculated MD-scores between conditions.

Micrococcal nuclease chromatin accessibility assay

MNase chromatin accessibility assays were largely performed as described (Infante et al. 2012). BEAS-2B cells were grown to confluence in 10-cm tissue culture dishes and treated with vehicle or dex (100 nM) for 10, 30, or 60 min. Crosslinking through nuclear isolation followed the protocol we used for ChIP. Nuclei were collected by centrifugation at 600*g* for 5 min at 4°C and resuspended in ice-cold nuclease digestion buffer (10 mM Tris-HCl at pH 8.0, 1 mM $CaCl_2$). MNase (10 Units/sample; New England Biolabs) was added, and reactions were incubated for 40 min at 37°C. Digestion was stopped by addition of an 8.6% SDS/7 mM EDTA solution, and crosslinks were reversed by adding Proteinase K (20 mg/mL; Life Technologies) and incubating 6 h at 65°C. DNA was purified, resuspended in 1× TE Buffer, and separated on a 2% agarose gel. Bands between 120 and 150 bp were excised and purified (QIAquick Gel Extraction kit; Qiagen). Tiled primer sets (Supplemental Table S3) with 80- to 120-bp amplicons and 40- to 60-bp overlap between adjacent sets were designed to span each region of interest. Chromatin accessibility was assayed using quantitative RT-PCR (Sasse et al. 2013). Primer efficiencies from genomic DNA amplification were used to normalize experimental Ct values. Assays were generally performed in biologic quadruplicate and repeated at least three times with qualitatively similar results.

Data access

All raw and processed sequencing data generated in this study have been submitted to the NCBI Gene Expression Omnibus (GEO; https://www.ncbi.nlm.nih.gov/geo/) under accession numbers GSE124916, GSE125623, and GSE135127.

Competing interest statement

R.D.D. is a founder of Arpeggio Biosciences.

Acknowledgments

This work was supported in part through the National Heart, Lung, and Blood Institute, NIH R01HL109557 (S.K.S., A.N.G.), F32HL136197 (V.K.), and National Institute of General Medical Sciences, NIH R01GM125871 (M.G., R.D.D.). The CU Boulder BioFrontiers Sequencing facility and the CU Anschutz Genomics Core, supported in part by the Genomics Shared Resource of the CU Cancer Center (P30CA046934), provided invaluable technical assistance. High Performance Computing resources (BioFrontiers Computing Core at CU Boulder) were funded by NIH 1S10OD012300.

References

Allen MA, Andrysik Z, Dengler VL, Mellert HS, Guarnieri A, Freeman JA, Sullivan KD, Galbraith MD, Luo X, Kraus WL, et al. 2014. Global analysis of p53-regulated transcription identifies its direct targets and unexpected regulatory mechanisms. *eLife* **3:** e02200. doi:10.7554/eLife.02200

Altonsy MO, Sasse SK, Phang TL, Gerber AN. 2014. Context-dependent cooperation between nuclear factor κB (NF-κB) and the glucocorticoid receptor at a *TNFAIP3* intronic enhancer: a mechanism to maintain negative feedback control of inflammation. *J Biol Chem* **289:** 8231–8239. doi:10.1074/jbc.M113.545178

Auphan N, DiDonato JA, Rosette C, Helmberg A, Karin M. 1995. Immunosuppression by glucocorticoids: inhibition of NF-κB activity through induction of IκB synthesis. *Science* **270:** 286–290. doi:10.1126/science.270.5234.286

Azofeifa JG, Dowell RD. 2017. A generative model for the behavior of RNA polymerase. *Bioinformatics* **33:** 227–234. doi:10.1093/bioinformatics/btw599

Azofeifa JG, Allen MA, Hendrix JR, Read T, Rubin JD, Dowell RD. 2018. Enhancer RNA profiling predicts transcription factor activity. *Genome Res* **28:** 334–344. doi:10.1101/gr.225755.117

Barnes PJ. 2006. Corticosteroids: the drugs to beat. *Eur J Pharmacol* **533:** 2–14. doi:10.1016/j.ejphar.2005.12.052

Castillo J, López-Rodas G, Franco L. 2017. Histone post-translational modifications and nucleosome organisation in transcriptional regulation: some open questions. *Adv Exp Med Biol* **966:** 65–92. doi:10.1007/5584_2017_58

Cheng Z, Teo G, Krueger S, Rock TM, Koh HW, Choi H, Vogel C. 2016. Differential dynamics of the mammalian mRNA and protein expression response to misfolding stress. *Mol Syst Biol* **12:** 855. doi:10.15252/msb.20156423

Chinenov Y, Gupte R, Rogatsky I. 2013. Nuclear receptors in inflammation control: repression by GR and beyond. *Mol Cell Endocrinol* **380:** 55–64. doi:10.1016/j.mce.2013.04.006

Clark AR, Belvisi MG. 2012. Maps and legends: the quest for dissociated ligands of the glucocorticoid receptor. *Pharmacol Ther* **134:** 54–67. doi:10.1016/j.pharmthera.2011.12.004

Cohen DM, Steger DJ. 2017. Nuclear receptor function through genomics: lessons from the glucocorticoid receptor. *Trends Endocrinol Metab* **28:** 531–540. doi:10.1016/j.tem.2017.04.001

Core LJ, Waterfall JJ, Lis JT. 2008. Nascent RNA sequencing reveals widespread pausing and divergent initiation at human promoters. *Science* **322:** 1845–1848. doi:10.1126/science.1162228

Cruz-Topete D, Cidlowski JA. 2015. One hormone, two actions: anti- and pro-inflammatory effects of glucocorticoids. *Neuroimmunomodulation* **22:** 20–32. doi:10.1159/000362724

Davis CA, Hitz BC, Sloan CA, Chan ET, Davidson JM, Gabdank I, Hilton JA, Jain K, Baymuradov UK, Narayanan AK, et al. 2018. The encyclopedia of DNA elements (ENCODE): data portal update. *Nucleic Acids Res* **46:** D794–D801. doi:10.1093/nar/gkx1081

De Bosscher K, Beck IM, Dejager L, Bougarne N, Gaigneaux A, Chateauvieux S, Ratman D, Bracke M, Tavernier J, Vanden Berghe W, et al. 2014. Selective modulation of the glucocorticoid receptor can distinguish between transrepression of NF-κB and AP-1. *Cell Mol Life Sci* **71:** 143–163. doi:10.1007/s00018-013-1367-4

Diehl AG, Boyle AP. 2016. Deciphering ENCODE. *Trends Genet* **32:** 238–249. doi:10.1016/j.tig.2016.02.002

Ewels P, Magnusson M, Lundin S, Käller M. 2016. MultiQC: summarize analysis results for multiple tools and samples in a single report. *Bioinformatics* **32:** 3047–3048. doi:10.1093/bioinformatics/btw354

Franco HL, Nagari A, Kraus WL. 2015. TNFα signaling exposes latent estrogen receptor binding sites to alter the breast cancer cell transcriptome. *Mol Cell* **58:** 21–34. doi:10.1016/j.molcel.2015.02.001

Gerber AN. 2015. Glucocorticoids and the lung. *Adv Exp Med Biol* **872:** 279–298. doi:10.1007/978-1-4939-2895-8_12

Gibbs J, Ince L, Matthews L, Mei J, Bell T, Yang N, Saer B, Begley N, Poolman T, Pariollaud M, et al. 2014. An epithelial circadian clock controls pulmonary inflammation and glucocorticoid action. *Nat Med* **20:** 919–926. doi:10.1038/nm.3599

Grant CE, Bailey TL, Noble WS. 2011. FIMO: scanning for occurrences of a given motif. *Bioinformatics* **27:** 1017–1018. doi:10.1093/bioinformatics/btr064

Guertin MJ, Zhang X, Coonrod SA, Hager GL. 2014. Transient estrogen receptor binding and p300 redistribution support a squelching mechanism for estradiol-repressed genes. *Mol Endocrinol* **28:** 1522–1533. doi:10.1210/me.2014-1130

Hah N, Danko CG, Core L, Waterfall JJ, Siepel A, Lis JT, Kraus WL. 2011. A rapid, extensive, and transient transcriptional response to estrogen signaling in breast cancer cells. *Cell* **145:** 622–634. doi:10.1016/j.cell.2011.03.042

Hargrove JL, Hulsey MG, Beale EG. 1991. The kinetics of mammalian gene expression. *Bioessays* **13:** 667–674. doi:10.1002/bies.950131209

Hoppenot D, Malakauskas K, Lavinskiene S, Sakalauskas R. 2015. p-STAT6, PU.1, and NF-κB are involved in allergen-induced late-phase airway inflammation in asthma patients. *BMC Pulm Med* **15:** 122. doi:10.1186/s12890-015-0119-7

Hua G, Zein N, Daubeuf F, Chambon P. 2019. Glucocorticoid receptor modulators CpdX and CpdX-D3 exhibit the same in vivo antiinflammatory activities as synthetic glucocorticoids. *Proc Natl Acad Sci* **116:** 14191–14199. doi:10.1073/pnas.1908258116

Hudson WH, Youn C, Ortlund EA. 2013. The structural basis of direct glucocorticoid-mediated transrepression. *Nat Struct Mol Biol* **20:** 53–58. doi:10.1038/nsmb.2456

Infante JJ, Law GL, Young ET. 2012. Analysis of nucleosome positioning using a nucleosome-scanning assay. *Methods Mol Biol* **833:** 63–87. doi:10.1007/978-1-61779-477-3_5

Jain D, Baldi S, Zabel A, Straub T, Becker PB. 2015. Active promoters give rise to false positive 'Phantom Peaks' in ChIP-seq experiments. *Nucleic Acids Res* **43:** 6959–6968. doi:10.1093/nar/gkv637

John S, Sabo PJ, Johnson TA, Sung MH, Biddie SC, Lightman SL, Voss TC, Davis SR, Meltzer PS, Stamatoyannopoulos JA, et al. 2008. Interaction of the glucocorticoid receptor with the chromatin landscape. *Mol Cell* **29:** 611–624. doi:10.1016/j.molcel.2008.02.010

Jubb AW, Young RS, Hume DA, Bickmore WA. 2016. Enhancer turnover is associated with a divergent transcriptional response to glucocorticoid in mouse and human macrophages. *J Immunol* **196:** 813–822. doi:10.4049/jimmunol.1502009

Jubb AW, Boyle S, Hume DA, Bickmore WA. 2017. Glucocorticoid receptor binding induces rapid and prolonged large-scale chromatin decompaction at multiple target loci. *Cell Rep* **21:** 3022–3031. doi:10.1016/j.celrep.2017.11.053

Kadiyala V, Sasse SK, Altonsy MO, Berman R, Chu HW, Phang TL, Gerber AN. 2016. Cistrome-based cooperation between airway epithelial glucocorticoid receptor and NF-κB orchestrates anti-inflammatory effects. *J Biol Chem* **291:** 12673–12687. doi:10.1074/jbc.M116.721217

Kampmann M, Bassik MC, Weissman JS. 2014. Functional genomics platform for pooled screening and generation of mammalian genetic interaction maps. *Nat Protoc* **9:** 1825–1847. doi:10.1038/nprot.2014.103

Kersul AL, Iglesias A, Ríos A, Noguera A, Forteza A, Serra E, Agustí A, Cosio BG. 2011. Molecular mechanisms of inflammation during exacerbations of chronic obstructive pulmonary disease. *Arch Bronconeumol* **47:** 176–183. doi:10.1016/S1579-2129(11)70043-X

Kim WB, Jerome D, Yeung J. 2017. Diagnosis and management of psoriasis. *Can Fam Physician* **63:** 278–285.

King EM, Chivers JE, Rider CF, Minnich A, Giembycz MA, Newton R. 2013. Glucocorticoid repression of inflammatory gene expression shows differential responsiveness by transactivation- and transrepression-dependent mechanisms. *PLoS One* **8:** e53936. doi:10.1371/journal.pone.0053936

Krebs W, Schmidt SV, Goren A, De Nardo D, Labzin L, Bovier A, Ulas T, Theis H, Kraut M, Latz E, et al. 2014. Optimization of transcription factor binding map accuracy utilizing knockout-mouse models. *Nucleic Acids Res* **42:** 13051–13060. doi:10.1093/nar/gku1078

Kulakovskiy IV, Vorontsov IE, Yevshin IS, Sharipov RN, Fedorova AD, Rumynskiy EI, Medvedeva YA, Magana-Mora A, Bajic VB, Papatsenko DA, et al. 2018. HOCOMOCO: towards a complete collection of transcription factor binding models for human and mouse via large-scale ChIP-Seq analysis. *Nucleic Acids Res* **46:** D252–D259. doi:10.1093/nar/gkx1106

Kulkarni HS, Elvington ML, Perng YC, Liszewski MK, Byers DE, Farkouh C, Yusen RD, Lenschow DJ, Brody SL, Atkinson JP. 2019. Intracellular C3 protects human airway epithelial cells from stress-associated cell death. *Am J Respir Cell Mol Biol* **60:** 144–157. doi:10.1165/rcmb.2017-0405OC

La Baer J, Yamamoto KR. 1994. Analysis of the DNA-binding affinity, sequence specificity and context dependence of the glucocorticoid receptor zinc finger region. *J Mol Biol* **239:** 664–688. doi:10.1006/jmbi.1994.1405

Lambert SA, Jolma A, Campitelli LF, Das PK, Yin Y, Albu M, Chen X, Taipale J, Hughes TR, Weirauch MT. 2018. The human transcription factors. *Cell* **175:** 598–599. doi:10.1016/j.cell.2018.09.045

Lim HW, Uhlenhaut NH, Rauch A, Weiner J, Hübner S, Hübner N, Won KJ, Lazar MA, Tuckermann J, Steger DJ. 2015. Genomic redistribution of GR monomers and dimers mediates transcriptional response to exogenous glucocorticoid in vivo. *Genome Res* **25:** 836–844. doi:10.1101/gr.188581.114

Loft A, Schmidt SF, Mandrup S. 2015. Modulating the genomic programming of adipocytes. *Cold Spring Harb Symp Quant Biol* **80:** 239–248. doi:10.1101/sqb.2015.80.027516

Love MI, Huber W, Anders S. 2014. Moderated estimation of fold change and dispersion for RNA-seq data with DESeq2. *Genome Biol* **15:** 550. doi:10.1186/s13059-014-0550-8

Masser AE, Kandasamy G, Kaimal JM, Andréasson C. 2016. Luciferase NanoLuc as a reporter for gene expression and protein levels in *Saccharomyces cerevisiae*. *Yeast* **33:** 191–200. doi:10.1002/yea.3155

McDowell IC, Barrera A, D'Ippolito AM, Vockley CM, Hong LK, Leichter SM, Bartelt LC, Majoros WH, Song L, Safi A, et al. 2018. Glucocorticoid receptor recruits to enhancers and drives activation by motif-directed binding. *Genome Res* **28:** 1272–1284. doi:10.1101/gr.233346.117

Meijsing SH. 2015. Mechanisms of glucocorticoid-regulated gene transcription. *Adv Exp Med Biol* **872:** 59–81. doi:10.1007/978-1-4939-2895-8_3

Morand EF. 2000. Corticosteroids in the treatment of rheumatologic diseases. *Curr Opin Rheumatol* **12:** 171–177. doi:10.1097/00002281-200005000-00002

Newton R, Shah S, Altonsy MO, Gerber AN. 2017. Glucocorticoid and cytokine crosstalk: feedback, feedforward, and co-regulatory interactions determine repression or resistance. *J Biol Chem* **292:** 7163–7172. doi:10.1074/jbc.R117.777318

Nicod LP, Kolls JK. 2015. Chair's summary: mechanisms of exacerbation of lung diseases. *Ann Am Thorac Soc* **12:** S112–S114. doi:10.1513/AnnalsATS.201503-139AW

Oh KS, Patel H, Gottschalk RA, Lee WS, Baek S, Fraser IDC, Hager GL, Sung MH. 2017. Anti-inflammatory chromatinscape suggests alternative mechanisms of glucocorticoid receptor action. *Immunity* **47:** 298–309.e5. doi:10.1016/j.immuni.2017.07.012

Pham CG, Bubici C, Zazzeroni F, Papa S, Jones J, Alvarez K, Jayawardena S, De Smaele E, Cong R, Beaumont C, et al. 2004. Ferritin heavy chain upregulation by NF-κB inhibits TNFα-induced apoptosis by suppressing reactive oxygen species. *Cell* **119:** 529–542. doi:10.1016/j.cell.2004.10.017

Quinlan AR, Hall IM. 2010. BEDTools: a flexible suite of utilities for comparing genomic features. *Bioinformatics* **26:** 841–842. doi:10.1093/bioinformatics/btq033

Rao NA, McCalman MT, Moulos P, Francoijs KJ, Chatziioannou A, Kolisis FN, Alexis MN, Mitsiou DJ, Stunnenberg HG. 2011. Coactivation of GR and NFKB alters the repertoire of their binding sites and target genes. *Genome Res* **21:** 1404–1416. doi:10.1101/gr.118042.110

Ratman D, Vanden Berghe W, Dejager L, Libert C, Tavernier J, Beck IM, De Bosscher K. 2013. How glucocorticoid receptors modulate the activity of other transcription factors: a scope beyond tethering. *Mol Cell Endocrinol* **380:** 41–54. doi:10.1016/j.mce.2012.12.014

Raundhal M, Morse C, Khare A, Oriss TB, Milosevic J, Trudeau J, Huff R, Pilewski J, Holguin F, Kolls J, et al. 2015. High IFN-γ and low SLPI mark severe asthma in mice and humans. *J Clin Invest* **125:** 3037–3050. doi:10.1172/JCI80911

Robinson JT, Thorvaldsdóttir H, Winckler W, Guttman M, Lander ES, Getz G, Mesirov JP. 2011. Integrative genomics viewer. *Nat Biotechnol* **29:** 24–26. doi:10.1038/nbt.1754

Ronchetti S, Migliorati G, Riccardi C. 2015. GILZ as a mediator of the anti-inflammatory effects of glucocorticoids. *Front Endocrinol* **6:** 170. doi:10.3389/fendo.2015.00170

Ruan H, Pownall HJ, Lodish HF. 2003. Troglitazone antagonizes tumor necrosis factor-α-induced reprogramming of adipocyte gene expression by inhibiting the transcriptional regulatory functions of NF-κB. *J Biol Chem* **278:** 28181–28192. doi:10.1074/jbc.M303141200

Sacta MA, Chinenov Y, Rogatsky I. 2016. Glucocorticoid signaling: an update from a genomic perspective. *Annu Rev Physiol* **78:** 155–180. doi:10.1146/annurev-physiol-021115-105323

Sacta MA, Tharmalingam B, Coppo M, Rollins DA, Deochand DK, Benjamin B, Yu L, Zhang B, Hu X, Li R, et al. 2018. Gene-specific mechanisms direct glucocorticoid-receptor-driven repression of inflammatory response genes in macrophages. *eLife* **7:** e34864. doi:10.7554/eLife.34864

Sasse SK, Mailloux CM, Barczak AJ, Wang Q, Altonsy MO, Jain MK, Haldar SM, Gerber AN. 2013. The glucocorticoid receptor and KLF15 regulate gene expression dynamics and integrate signals through feed-forward circuitry. *Mol Cell Biol* **33:** 2104–2115. doi:10.1128/MCB.01474-12

Sasse SK, Altonsy MO, Kadiyala V, Cao G, Panettieri RA Jr., Gerber AN. 2016. Glucocorticoid and TNF signaling converge at A20 (TNFAIP3) to repress airway smooth muscle cytokine expression. *Am J Physiol Lung Cell Mol Physiol* **311:** L421–L432. doi:10.1152/ajplung.00179.2016

Sasse SK, Kadiyala V, Danhorn T, Panettieri RA Jr, Phang TL, Gerber AN. 2017. Glucocorticoid receptor ChIP-seq identifies PLCD1 as a KLF15 target that represses airway smooth muscle hypertrophy. *Am J Respir Cell Mol Biol* **57:** 226–237. doi:10.1165/rcmb.2016-0357OC

Schmidt SF, Larsen BD, Loft A, Mandrup S. 2016. Cofactor squelching: artifact or fact? *Bioessays* **38:** 618–626. doi:10.1002/bies.201600034

Schuliga M. 2015. NF-κB signaling in chronic inflammatory airway disease. *Biomolecules* **5:** 1266–1283. doi:10.3390/biom5031266

Schwanhäusser B, Busse D, Li N, Dittmar G, Schuchhardt J, Wolf J, Chen W, Selbach M. 2011. Global quantification of mammalian gene expression control. *Nature* **473:** 337–342. doi:10.1038/nature10098

So AY, Chaivorapol C, Bolton EC, Li H, Yamamoto KR. 2007. Determinants of cell- and gene-specific transcriptional regulation by the glucocorticoid receptor. *PLoS Genet* **3:** e94. doi:10.1371/journal.pgen.0030094

Step SE, Lim HW, Marinis JM, Prokesch A, Steger DJ, You SH, Won KJ, Lazar MA. 2014. Anti-diabetic rosiglitazone remodels the adipocyte transcriptome by redistributing transcription to PPARγ-driven enhancers. *Genes Dev* **28:** 1018–1028. doi:10.1101/gad.237628.114

Swinstead EE, Miranda TB, Paakinaho V, Baek S, Goldstein I, Hawkins M, Karpova TS, Ball D, Mazza D, Lavis LD, et al. 2016. Steroid receptors reprogram FoxA1 occupancy through dynamic chromatin transitions. *Cell* **165:** 593–605. doi:10.1016/j.cell.2016.02.067

Teytelman L, Thurtle DM, Rine J, van Oudenaarden A. 2013. Highly expressed loci are vulnerable to misleading ChIP localization of multiple unrelated proteins. *Proc Natl Acad Sci* **110:** 18602–18607. doi:10.1073/pnas.1316064110

Toropainen S, Niskanen EA, Malinen M, Sutinen P, Kaikkonen MU, Palvimo JJ. 2016. Global analysis of transcription in castration-resistant prostate cancer cells uncovers active enhancers and direct androgen receptor targets. *Sci Rep* **6:** 33510. doi:10.1038/srep33510

Tripodi IJ, Allen MA, Dowell RD. 2018. Detecting differential transcription factor activity from ATAC-seq data. *Molecules* **23:** 1136. doi:10.3390/molecules23051136

Tsompana M, Buck MJ. 2014. Chromatin accessibility: a window into the genome. *Epigenetics Chromatin* **7:** 33. doi:10.1186/1756-8935-7-33

Uhlenhaut NH, Barish GD, Yu RT, Downes M, Karunasiri M, Liddle C, Schwalie P, Hübner N, Evans RM. 2013. Insights into negative regulation by the glucocorticoid receptor from genome-wide profiling of inflammatory cistromes. *Mol Cell* **49:** 158–171. doi:10.1016/j.molcel.2012.10.013

Vandewalle J, Luypaert A, De Bosscher K, Libert C. 2018. Therapeutic mechanisms of glucocorticoids. *Trends Endocrinol Metab* **29:** 42–54. doi:10.1016/j.tem.2017.10.010

Vettorazzi S, Bode C, Dejager L, Frappart L, Shelest E, Klaßen C, Tasdogan A, Reichardt HM, Libert C, Schneider M, et al. 2015. Glucocorticoids limit acute lung inflammation in concert with inflammatory stimuli by induction of SphK1. *Nat Commun* **6:** 7796. doi:10.1038/ncomms8796

Visel A, Blow MJ, Li Z, Zhang T, Akiyama JA, Holt A, Plajzer-Frick I, Shoukry M, Wright C, Chen F, et al. 2009. ChIP-seq accurately predicts tissue-specific activity of enhancers. *Nature* **457:** 854–858. doi:10.1038/nature07730

Voss TC, Schiltz RL, Sung MH, Yen PM, Stamatoyannopoulos JA, Biddie SC, Johnson TA, Miranda TB, John S, Hager GL. 2011. Dynamic exchange at regulatory elements during chromatin remodeling underlies assisted loading mechanism. *Cell* **146:** 544–554. doi:10.1016/j.cell.2011.07.006

Wang JC, Stromstedt PE, Sugiyama T, Granner DK. 1999. The phosphoenolpyruvate carboxykinase gene glucocorticoid response unit: identification of the functional domains of accessory factors HNF3 β (hepatic nuclear factor-3 β) and HNF4 and the necessity of proper alignment of their cognate binding sites. *Mol Endocrinol* **13:** 604–618. doi:10.1210/mend.13.4.0269

Yang L, Fliegauf M, Grimbacher B. 2014. Hyper-IgE syndromes: reviewing PGM3 deficiency. *Curr Opin Pediatr* **26:** 697–703. doi:10.1097/MOP.0000000000000158

Zhang Y, Liu T, Meyer CA, Eeckhoute J, Johnson DS, Bernstein BE, Nusbaum C, Myers RM, Brown M, Li W, et al. 2008. Model-based Analysis of ChIP-Seq (MACS). *Genome Biol* **9:** R137. doi:10.1186/gb-2008-9-9-r137

Received January 18, 2019; accepted in revised form September 6, 2019.